J Solid State Electrochem (2005) 9: 581–589
DOI 10.1007/s10008-004-0604-z

ORIGINAL PAPER

Nataliya V. Roznyatovskaya · Sergey Yu. Vassiliev
Alexander I. Yusipovich · Galina A. Tsirlina
Vladimir V. Roznyatovskii

Aqueous electrochemistry of binuclear copper complex with Robson-type ligand: dissolved versus surface-immobilized reactant

Received: 13 August 2004 / Revised: 18 August 2004 / Accepted: 9 September 2004 / Published online: 21 January 2005

Abstract The electrochemical behaviour of binuclear copper complex with Robson-type ligand $[Cu_2L]Cl_2$ in aqueous medium is studied by cyclic voltammetry at highly oriented pyrolytic graphite, glassy carbon and gold electrodes. The overall reduction from solution of this reactant is found to be irreversible resulting in metallic copper formation. It is also complicated by chemical transformations of Cu(I) containing species. When attached to carbon support, $[Cu_2L]Cl_2$ is redox active in aqueous medium in the same potential range. The reduction is more reversible if reactant is immobilized at HOPG surface, and is in general agreement with reversible copper demetallation scheme. For dissolved reactant, the contribution of surface-attached species is screened by predominating voltammetric response of irreversible reduction. These conclusions are supported by data on the reduction of free protonated ligand and its hydrolysis products. Ex situ STM is applied to characterize electrode surfaces modified by $[Cu_2L]Cl_2$. Adsorbate monolayer of periodic structure is observed at highly oriented pyrolytic graphite (HOPG). Adsorption is more disordered at GC and less strong at polycrystalline gold support.

Keywords Binuclear copper macrocyclic complex · STM images · Cyclic voltammetry · Electroreduction · Aqueous medium

Introduction

Template binuclear complexes of transition metals with Robson-type ligands [1–3] give a chance to discover new electrocatalytic systems with unusual mediating behaviour [4]. For aqueous systems, future applications of these compounds are limited by their low solubility and poorly studied electrochemistry.

We report below the study of $[Cu_2L]Cl_2$ (Fig. 1a, L is the product of [2 + 2] condensation of 2,6-diformyl-4-*t*-butylphenol and 1,3-diaminopropane), a representative of this group which demonstrates satisfactory solubility in aqueous medium at room temperature (millimolar range), but rather slow dissolution kinetics. General peculiarities of $[Cu_2L]Cl_2$ aqueous electrochemistry are reported in our recent paper [5]. The most unusual feature discovered in [5] is a single wave which corresponds to four electron destructive reduction with formation of metallic copper and precedes the reduction of ligand (in contrast to well-separated single electron waves observed in aprotic solvents [6–9]).

Further investigation of redox behaviour of $[Cu_2L]Cl_2$ immobilized at solid electrode materials is crucial for estimating electrocatalytic prospects of reactants under study because one cannot expect any mediating ability for chemically irreversible redox process. It is also important for future understanding of the nature of the abovementioned four-electron wave (which evidently consists of coalesced waves).

Recent attempt to study the redox behaviour of solid mechanically attached binuclear and tetranuclear copper complexes with Robson-type ligand in aqueous solutions [10] revealed that these reactants undergoes reversible demetallation in the course of reduction process and reforming upon oxidation cycle. On the other hand, the insolubility of reactants under study in Ref. [10] in aqueous medium prevents from direct comparing of electroreduction features of dissolved and surface-immobilized species using the same electrode material and solvent.

To provide such comparison we studied the redox properties of soluble $[Cu_2L]Cl_2$ in aqueous medium at highly oriented pyrolytic graphite (HOPG), glassy carbon (GC) and polycrystalline gold electrodes. The spe-

N. V. Roznyatovskaya (✉) · S. Y. Vassiliev
A. I. Yusipovich · G. A. Tsirlina · V. V. Roznyatovskii
Department of Electrochemistry, Faculty of Chemistry,
Moscow State University, Leninskie Gory 1-str.3,
Moscow, 119992 Russia
E-mail: nat.rozn@nmr.chem.msu.su

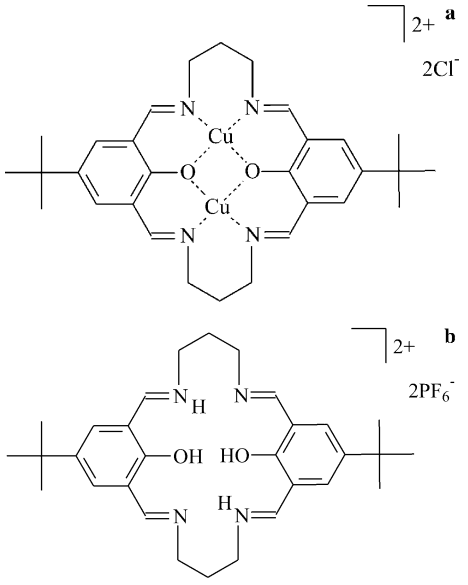

Fig. 1 Schematic structure of $[Cu_2L]Cl_2$ (**a**) and the ligand compound $[H_4L](PF_6)_2$ (**b**)

cific features of $[Cu_2L]Cl_2$ immobilization at HOPG, GC and gold supports was investigated by ex situ STM technique. As the $[Cu_2L]Cl_2$ reduction is closely related to the free ligand redox behaviour, the DC-polarographic data for this reactant and free ligand protonated salt ($[H_4L](PF_6)_2$, Fig. 1b) are also compared.

Experimental

Chemicals

$CH_3COONa{\cdot}3H_2O$ and glacial acetic acid (pure per analysis, Merck) were used for preparation of buffer supporting solution. All solutions were prepared with twice deionized and filtered water (Milli-Q and Elix purification system).

Reactants

$[Cu_2L]Cl_2{\cdot}H_2O$ was prepared using well-developed procedure for template condensation [3, 11], recrystallized from water and characterized by elemental analysis (calculated for $C_{30}H_{38}N_4O_2Cl_2Cu_2{\cdot}H_2O$ (%): C, 51.28; H, 5.73; N, 7.93; found: C, 51.6; H, 5.4; N, 7.9), IR analysis ((Nujol) ν (cm^{-1}): 1,640 (C=N), 1,330 (C-O), 1,570 (C=C)), TGA (decomposition point is 326°C (in air), incombustible residue calculated for CuO: 22.6%, found: 19.4%).

The protonated salt of free ligand was synthesized according to procedure [12], then was twice recrystallized from the mixture of acetonytrile and diethyl ether and characterized by elemental analysis (calculated for $C_{30}H_{42}N_4O_2P_2F_{12}$ (%): C, 46.16; H, 5.42; N, 7.18; found: C, 45.8; H, 5.6; N, 7.2), ^{1}H NMR (300 MHz, acetone d_6: $\delta = 1.2$ (18H, s), 2.55 (4H, m), 4.28 (8H, d), 7.7 (4H, s), 8.68 (4H, d), 13.75 (br s)).

Instrumentation

Cyclic voltammograms were recorded using an EG&G PARC 273A potentiostat:galvanostat controlled by software running on a PC. The measurements were carried out in a three-electrode glass cell with separated compartments using a saturated calomel electrode (SCE) as the reference connected with a cell via Luggin capillary with saturated KCl salt bridge and a Pt plate as the auxiliary electrode. The working electrode was either a HOPG (ZH, NTMDT, Russia), or a GC (Alfa Aesar) or gold wire.

DC-polarography was carried out on DME with the mercury flow rate of 0.91 mg s^{-1} and open circuit drop life time of 8.1 s under the same conditions as described in Ref. [5]. Polarogramms are presented with subtraction of background currents. All potentials below are referred to SCE.

For STM characterization, a homemade LitScan device was applied. Base voltage and base current were specially chosen for each sample to obtain better resolution. This choice was based on preliminary measurement of various tunneling spectra [13].

Procedures

Before taking measurements, the working electrodes were pretreated with concentrated sulfuric acid for 3–5 min (GC electrode) or with a hot mixture of concentrated nitric and hydrochloric acids (1:3) (gold wire electrode) and rinsed with deionized water. The working surface of HOPG was cleaved mechanically by adhesive tape before each series of experiments. In order to eliminate the contribution of lateral faces in overall capacitance of HOPG electrode, before CV measurement these sides of HOPG were covered with chemically pure paraffin. A textured film of Au on mica was annealed at 800°C.

All solutions of $[Cu_2L]Cl_2$ (0.33 mM) for CV experiments were supported with acetate buffer (0.1 M pH 6.0) and were deaerated with argon during at least 25 min before measurements. The cyclic voltammograms in solutions under study were registrated after CVs in supporting buffer solution, without additional pretreatment of the working electrode, except for the case of $[Cu_2L]Cl_2$ immobilized onto HOPG surface. Measured at HOPG, GC and gold electrodes CVs of $[Cu_2L]Cl_2$ became stabilized from the second scan except for scan rate 0.5 V s^{-1} at HOPG.

For immobilization of $[Cu_2L]Cl_2$ at HOPG support a droplet of 20–40 µl of $[Cu_2L]Cl_2$ solution (0.085 mM) in water was deposited on a freshly cleaved HOPG surface and was allowed to dry in air under ambient conditions. The same immobilization procedure was applied in STM

experiments at HOPG, GC and gold supports. The quantity of immobilized species was estimated on the basis of crystallographic data for $[Cu_2L]Cl_2$ molecule [11] to obtain several monolayers per geometric surface, area of HOPG electrode. To study redox activity of $[Cu_2L]Cl_2$ attached to GC surface GC electrode was immersed into 0.33 mM buffered solution of $[Cu_2L]Cl_2$ for ca. 30 min before CV measurements in supporting solution.

For DC-polarographic measurements the solutions of $[H_4L](PF_6)_2$, 2,6-diformyl-4-*t*-butylphenol and $[Cu_2L]Cl_2$ (0.2 mM) were prepared in an acetate buffer (0.1 M pH 6.0).

Results and discussion

Comparative electrochemical study of $[Cu_2L]Cl_2$ and $[H_4L](PF_6)_2$ in solution

The experiments on electroreduction of binuclear complexes of Robson-type ligands are in close connection with the redox behaviour of their free macrocyclic ligand and are especially crucial if the reduction of metal complex leads to demetallation. Possible potential range of the ligands redox activity in organic solvents was estimated on the basis of data on electroreduction of their complexes with redox inactive ions (for example Zn(II)). Synthesis and isolation of metal-free Schiff-base macrocycles were poorly available for a long time since the first synthesis of binuclear metal complexes of Robson-type ligands [12]. As far as we know the electrochemistry of free ligand corresponding to the $[Cu_2L]Cl_2$ or its protonated salt was never reported.

In accordance with our previous data [5] the reduction of $[Cu_2L]Cl_2$ by preparative electrolysis at mercury pool electrode leads to metallic copper and free ligand formation with parallel or subsequent hydrolysis in aqueous medium (pH 6.0). These data correspond to potential region of the first polarographic wave (Fig. 2, solid curve). The subsequent waves are surely related to the reduction of organic species, which is discussed for the first time in this section.

The dissolution of $[H_4L](PF_6)_2$ in acetate buffer (11.7 mg of ligand salt for 100 ml, pH 6.0) is found to be complicated by low solubility of the ligand itself or likely its hydrolysis products (one of them being 2,6-diformyl-4-*t*-butylphenol denoted as dfph). Hence, to prepare the solution which would model the species associated with $[H_4L]^{2+}$ in aqueous medium, undissolved portion was filtered out and the resulting solution, denoted here as solution of $[H_4L](PF_6)_2$, is studied by DC-polarography at dropping mercury electrode. Comparing polarograms of this solution and the saturated solution of dfph (Fig. 2, dashed and dotted curves, respectively) the following features are to be noted. Both curves are characterized by two waves, but the fraction of the first wave limiting current ($E_{1/2}$ ca. −0.9 V) in overall response for solution of $[H_4L](PF_6)_2$ is lower than those for solution of dfph. The reduction in the solution of $[H_4L](PF_6)_2$ starts at −0.85 V that is ca. 0.1 V less negative than the

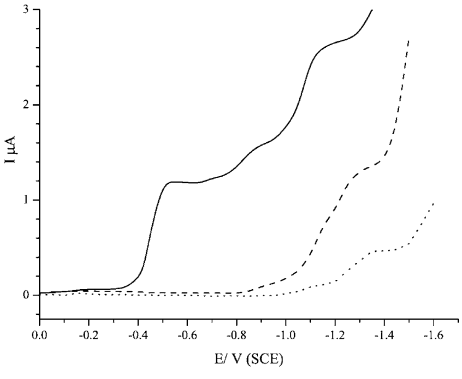

Fig. 2 DC polarographic curves recorded in acetate buffer (pH 6.0) solutions of: *solid line* 0.2 mM of $[Cu_2L]Cl_2$, *dashed line* partly hydrolyzed solution of $[H_4L](PF_6)_2$ (see text), *dotted line* saturated 2,6-diformyl-4-*t*-butylphenol

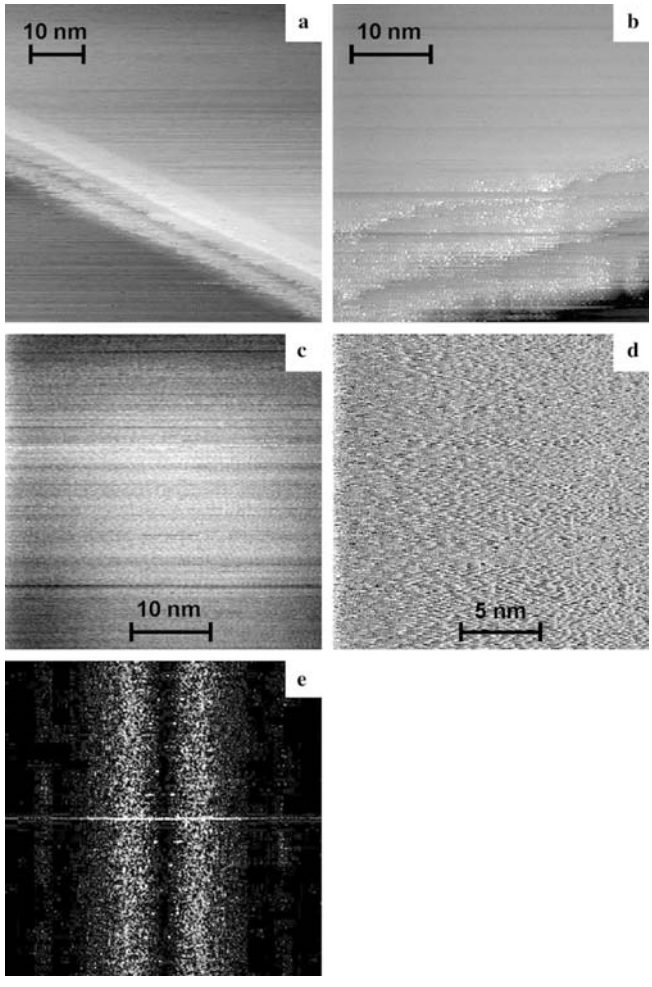

Fig. 3 STM data for HOPG: **a** bare support; **b**–**d** modified surface (20 μl of 85 μM $[Cu_2L]Cl_2$, ca. five monolayers, with subsequent washing), **e** Fourier transformed spectra obtained from (**d**), the same scale as for (**d**). Modes: base voltage 0.15 V, base current 130 pA, **a**–**c** constant current mode, **d** constant height mode

onset of dfph reduction. These facts may be explained by the presence of another redox active product of $[H_4L]^{2+}$ hydrolysis (besides dfph) in the solution under study, or by redox activity of non-destructed protonated ligand.

The polarogram of $[Cu_2L]Cl_2$ reduction (solid curve in Fig. 2) demonstrates three waves at the same potential region. Compared to the curve for the solution of $[H_4L](PF_6)_2$ the second wave of $[Cu_2L]Cl_2$ commence at even more positive potentials (ca. −0.7 V) and the onset of the third wave (ca. −1 V) is close to the onset of dfph reduction. This observation contradicts the simplified assumption of ligand destruction starting only after transfer of four electrons. More realistic hypothesis is the formation of $[H_4L]^{2+}$ hydrolysis products in the course of earlier chemical steps, i.e. after formation of Cu(I) containing species.

$[Cu_2L]Cl_2$ interaction with solid surfaces as observed by STM

Obvious STM manifestations of $[Cu_2L]Cl_2$ strong adsorption were obtained for HOPG. After thorough washing some portion of initially deposited reactant was deleted, but the difference of bare (Fig. 3a) and modified HOPG surfaces was still visible. Adsorbate monolayer of periodic structure was imaged under both constant current (Fig. 3c) and constant height (Fig. 3d) modes. To estimate the geometry of 2D adlattice, Fourier transformation was applied (Fig. 3e). Disordered hexagonal cell with parameters ca. 1.25 nm×1.15 nm^2 and 126° angle can be assumed on the basis of this analysis. These parameters do not contradict the molecular size and 3D cell parameters (0.7×1.9×1.7 nm^3) [11]. The unit cell area is close to the areas of some 2D projections of crystal unit cell.

Accumulation of excess quantity of $[Cu_2L]Cl_2$ was found in the vicinity of HOPG steps (compare Fig. 3a, b). This phenomena was most probably responsible for complications met when cleaving HOPG surface after previous immobilization.

Interpretation of STM data for GC surface is much more difficult because of inhomogeneous morphology of bare support (Fig. 4a). The majority of morphological features remain the same after immobilization (Fig. 4b, c). More degraded images resulting from surface modification make it possible to assume the formation of $[Cu_2L]Cl_2$ monolayer or even thicker films. It is rather probable that $[Cu_2L]Cl_2$ forms nm-size fragments which are distributed between larger native fragments of GC (Fig. 4c). Fourier analysis fails to extract any periodic structure, which can result from less strong adsorption (as compared to HOPG). However, one cannot exclude that nm-size disorder of GC support is responsible for this fail. Basically, we can conclude STM manifestations of $[Cu_2L]Cl_2$ adsorption on GC.

When depositing ca. 10 monolayers of $[Cu_2L]Cl_2$ on gold we observe the fragments of several nm size (compare Fig. 5a, b) which can be interpreted as nanocrystals. These fragments disappear after washing (Fig. 5c), and no manifestations of residual adsorbate are observed. The unclear shape of gold atomic steps after washing gives evidence of $[Cu_2L]Cl_2$-induced

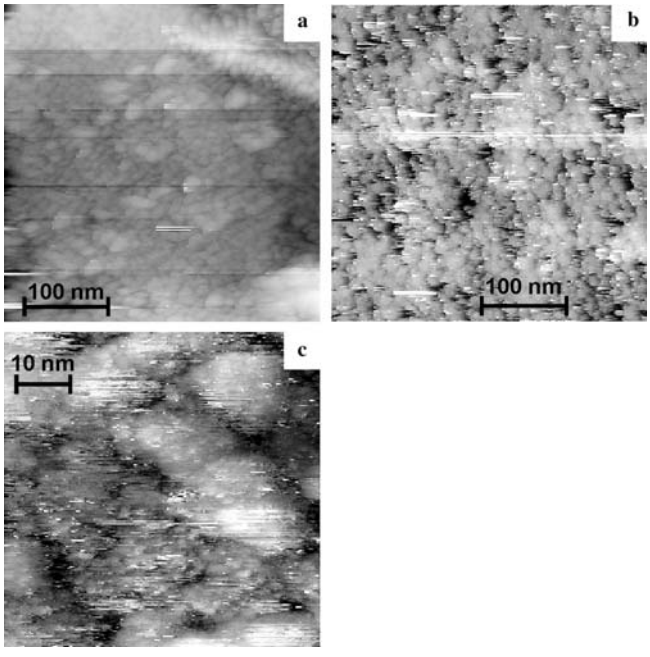

Fig. 4 STM data for GC: **a** bare support, **b**, **c** modified surface (20 µl of 85 µM $[Cu_2L]Cl_2$, ca. five monolayers). Base voltage −1.0 V, base current 300 pA

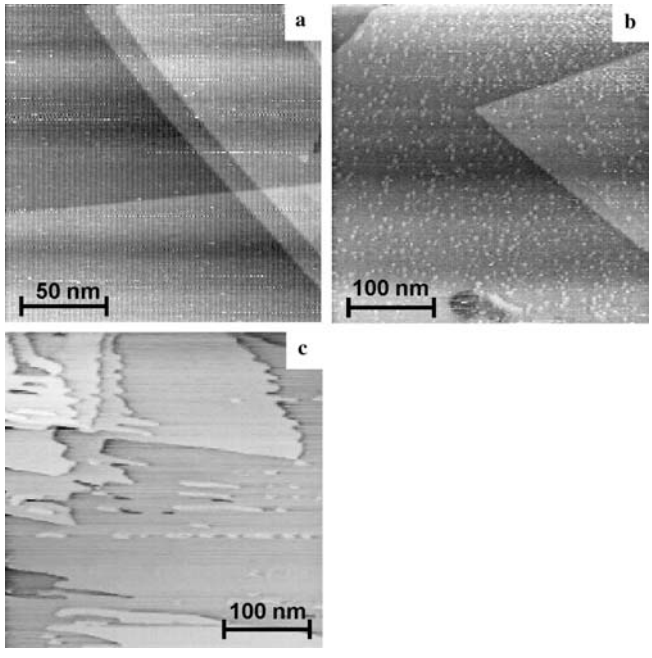

Fig. 5 STM data for Au film on mica: **a** bare support, **b** modified surface (40 µl of 85 µM $[Cu_2L]Cl_2$, ca. 10 monolayers), **c** modified surface after washing. Base voltage 0.7 V, base current 700 pA

reconstruction, which phenomenon is out of frames of this study.

In general STM demonstrates the following difference in $[Cu_2L]Cl_2$ interaction with solid surfaces under study. The most strong and ordered adsorption takes place on HOPG. GC also seems to be able to adsorb the reactant, but adlayers are more disordered. Adlayers of $[Cu_2L]Cl_2$ formed on carbon supports remain stable after washing. Contrary, for gold no exact evidence of $[Cu_2L]Cl_2$ adsorbate remaining at the surface after washing is found.

Electrochemical behaviour of dissolved $[Cu_2L]Cl_2$ at solid electrodes

Typical cyclic voltammograms of $[Cu_2L]Cl_2$ in aqueous solutions are presented in Fig. 6. At CVs recorded varying cathodic boundary potential (E_{lim}) from −0.5 to −1 V the most pronounced reduction process (denoted below C1) is observed at all electrode materials under discussion. The presence of either plateau or peak corresponding to C1 process at gold electrode seems to be dependent on the electrode pretreatment. The onset of the reduction (C1) for $[Cu_2L]Cl_2$ at solid electrodes is close to that found in DC-polarography experiment on mercury (solid curve in Fig. 2).

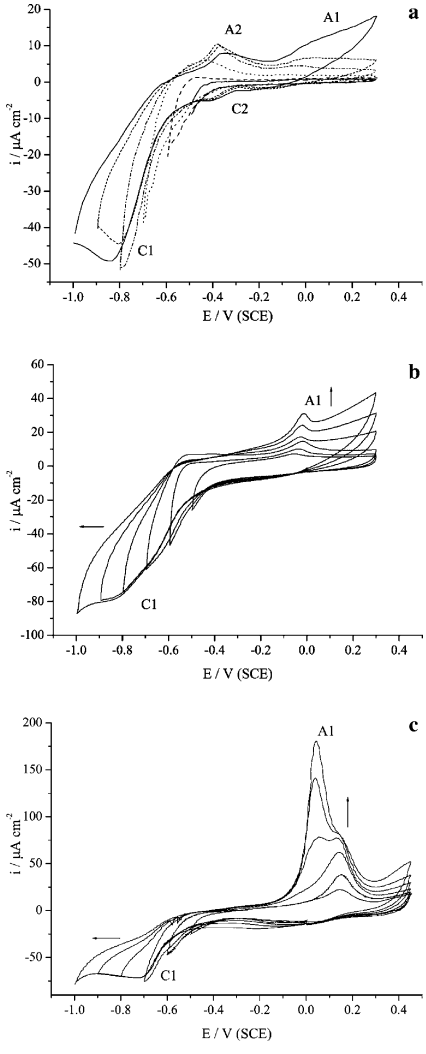

Fig. 6 Cyclic voltammograms for 0.33 mM solution of $[Cu_2L]Cl_2$ (pH 6.0) recorded with cathodic limits −0.5, −0.6, −0.7, −0.8, −0.9 and −1 V (scan rate 0.05 V s^{-1}) at: **a** HOPG (0.49 cm^2), **b** GC (2.3 cm^2), **c** gold electrode (0.16 cm^2) (*arrows* denote a tendencies resulting from the shift of cathodic limit)

All voltammetric curves under discussion (Fig. 6) show an anodic response in the vicinity of potential ca. 0 V, denoted below as A1. The deeper is the cathodic process C1, the higher charges pass in the course of anodic A1 process giving evidence of coupling of these processes. Interrelation of C1 and A1 is especially pronounced for gold electrode (Fig. 6c). A coalesced nature of peak corresponding to A1 is associated with desorption of copper adatoms (peak at ca. 0.15 V) and copper overlayer (peak at ca. 0 V) [5].

The charge spent for adatoms oxidation is always lower as compared to the charge of complete monolayer desorption (420 $\mu C\ cm^{-2}$) and remains constant (ca. 270 $\mu C\ cm^{-2}$) even when the second anodic peak (at 0 V) is already observed. Further copper accumulation appears to be possible only in the overlayer. Partial surface blocking by another adsorbate can be responsible for preventing the formation of complete copper monolayer. We assume this adsorbate to be organic ligand and/or its fragments.

Though an anodic response A1 is less pronounced at CVs of $[Cu_2L]Cl_2$ recorded at HOPG and GC electrodes, its charge also correlates with the charge spent for reduction C1 (Fig. 6a, b). HOPG electrode is likely to be more sensitive (than GC or gold) to possible irreversible processes resulting in the changes of the surface state in the course of $[Cu_2L]Cl_2$ reduction. So with subsequent shifting of E_{lim} from −0.5 to −1 V the CVs at HOPG undergo less distinct changes. The deposition and desorption of copper on GC are studied in detail in recent Ref. [14]. No evidence of adatoms formation is observed, and nucleation and desorption kinetics is also found to differ from known for noble metal electrodes. Complications of cuprous ions reduction and stripping experiments in neutral solutions is found at carbon microelectrode [15]. Thus, the difference of anodic peaks associated with process A1 at carbon (Fig. 6a, b) and gold (Fig. 6c) electrodes agrees well with the specific properties of copper deposits at these materials.

In contrast to CVs at other electrodes, voltammograms for HOPG demonstrate an additional redox feature corresponding to cathodic process C2 and associated anodic peak of process A2 (Fig. 6a). These peaks are observed at CV, when E_{lim} is −0.8 V or more negative. Possible nature of C2 and A2 is discussed below. The voltammetric data on $[Cu_2L]Cl_2$ reduction at HOPG, GC and gold electrodes are summarized in Table 1.

To exclude the potential region of the ligand redox activity (polarographic waves at potentials more neg-

Table 1 Peak potentials or potential ranges (V/SCE) of redox process (denoted in brackets) observed at CVs (0.1 M acetate buffer pH 6.0): for dissolved $[Cu_2L]Cl_2$, for immobilized $[Cu_2L]Cl_2$

Scan direction	Electrode				
	HOPG		GC		Gold
	Dissolved $[Cu_2L]Cl_2$	Immobilized $[Cu_2L]Cl_2$	Dissolved $[Cu_2L]Cl_2$	Immobilized $[Cu_2L]Cl_2$	Dissolved $[Cu_2L]Cl_2$
Cathodic	(C1) −0.7 to −1[a] (C2) −0.4[a]	(C2) −0.6	(C1) −0.75 to −0.9	(C1) −0.65[e]	(C1) −0.7 to −0.9
Anodic	(A1) 0 to 0.2[b] (A2) −0.4[a] −0.25[c]	(A1) 0 (A2) −0.5	(A1) 0	(A1) 0	(A1) 0 to 0.3[d]
	(A3) −0.5[f]		(A3) −0.5[c]		

[a]Dependent on the number of preceding cycles and/or scan rates
[b]Peak/coalesced peak shaped only at 0.010–0.025 V s^{-1}
[c]Observed at scan rates higher than 0.050 V s^{-1}
[d]Two coalesced peaks
[e]Indistinct peak
[f]Observed only in the potential range from 0.3 to −0.7 V; at scan rates 0.025 to 0.05 V s^{-1} a coalesced peak at −0.4 V is detected

ative than −0.7 V, solid curve in Fig. 2) the redox behaviour of $[Cu_2L]Cl_2$ at carbon electrode materials is studied in the range from 0.3 to −0.7 V. CVs at HOPG and GC of $[Cu_2L]Cl_2$ at different scan rates for potential being swept in this restricted region (Fig. 7) demonstrate an important additional feature. Besides the peaks associated with C1 and A1 a broad anodic voltammetric response A3 appears in the region ca. −0.5 V at scan rate exceeding 0.025 V s^{-1}. This peak potential slightly shifts with scan rate at HOPG (Fig. 7a); less distinct peak at −0.55 is found at GC at

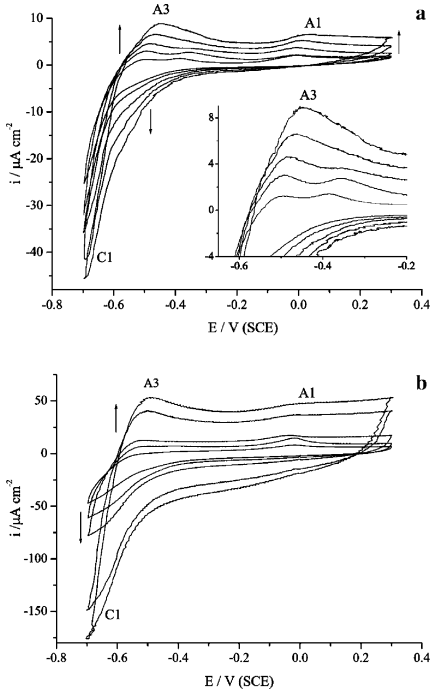

Fig. 7 Cyclic voltammograms for 0.33 mM solution of $[Cu_2L]Cl_2$ (pH 6.0) recorded in the restricted potential region ($E_{lim} = -0.7$ V) at: **a** HOPG (0.42 cm^2), scan rates 0.025, 0.05, 0.1, 0.2 and 0.35 V s^{-1} (*inset*: the enlarged fragment of CVs), **b** GC (2.3 cm^2) electrode, scan rates from 0.025, 0.05, 0.1, 0.35 and 0.5 V s^{-1} (*arrows* indicate the tendencies resulting from increase of scan rate)

scan rate higher than 0.05 V s^{-1} (Fig. 7b). Because of rather negative potential the anodic process A3 cannot be assigned to oxidation of copper metal and should be considered as manifestation of redox activity of intermediate Cu(I) containing product of $[Cu_2L]Cl_2$ reduction. Since this peak is observed only when the reduction process is less deep (that is cathodic E_{lim} is more positive than −0.7 V) and at scan rate is not too low, an intermediate chemical reaction of finite rate is supposed to take place. Taking into account the features of $[Cu_2L]Cl_2$ reduction at DME the fact that chemical step affects the intermediate product of reactant reduction is rather plausible.

The coalesced nature of peak assigned to process A3 (Fig. 7a, inset) is more evident at scan rates 0.025–0.05 V s^{-1}. Thus the peak at ca. −0.4 V (Fig. 7a) cannot be assigned uniquely to process A3, especially taking into account the presence of responses (A2) and (C2) at the same potential at HOPG (Fig. 6a). On the other hand, the peak at ca. −0.5 V (another component of coalesced response (A3)) is strongly dependent on scan rate and is detected at both HOPG and GC electrodes only if E_{lim} remains in the region of the first polarographic wave.

The peaks assigned to processes C2 and A2 are most pronounced at CVs of $[Cu_2L]Cl_2$ when the potential is swept from 0 to −1 V (Fig. 8a). It is to be emphasized that the CVs for $[Cu_2L]Cl_2$ at HOPG electrode are sensitive to the sequence of scan rates, E_{lim} values and the number of preceding cycles. Such specific feature of HOPG can be explained by accumulation of solid product (metallic copper) at the surface in the course of reactant reduction and copper incomplete dissolution at certain scan rates. In particular, C2/A2 redox process is very sensitive to this cycling history, and its small response is sometimes hardly detectable at low scan rates (Fig. 8a). The dependence of peak current on scan rate is found to be linear for the peak associated with A2 and deviates from linear (to lower current values) for the peak associated with C2. This type of current dependence

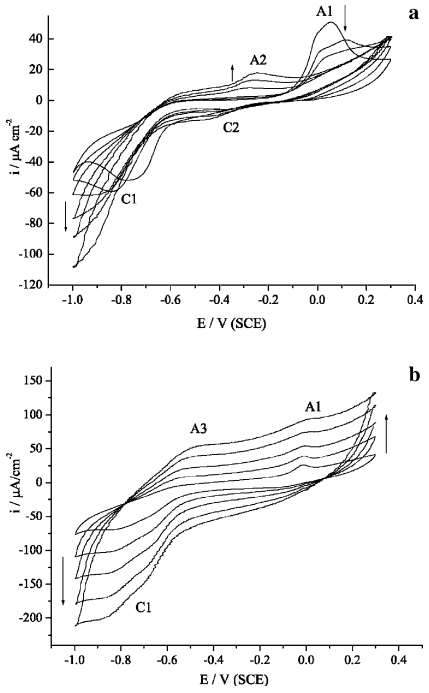

Fig. 8 Cyclic voltammograms for 0.33 mM solution of $[Cu_2L]Cl_2$ (pH 6.0) recorded in a wide potential region ($E_{lim} = -1$ V) at: **a** HOPG (0.42 cm^2), scan rates 0.01, 0.025, 0.05, 0.2, 0.35 and 0.5 V s^1, **b** GC electrode (2.3 cm^2), scan rates 0.05, 0.1, 0.2, 0.35 and 0.5 V s^{-1} (*arrows* indicate the tendencies resulting from increase of scan rate)

on scan rate can evidence the presence of quasi-equilibrium redox transition for adsorbed species which occurs in parallel with dissolved $[Cu_2L]Cl_2$ reduction.

The evolution of CVs at HOPG manifests the following features. At slow scan rates (0.01–0.05 V s^{-1}) the CV curves at HOPG demonstrate a broad cathodic peak corresponding to C1 ($E_{p,C1}$ shifts from −0.75 to −1 V). The peak current $I_{p,C1}$ slightly decreases in subsequent potential cycles at high scan rates (0.35–0.5 V s^{-1}). It is coupled with coalesced anodic peaks in the potential range from 0 to 0.1 V (process A1). With an increase of scan rate the anodic peak current $I_{p,A1}$ decreases, and a pair of cathodic (C2) and anodic (A2) peaks is detected (from −0.45 to −0.25 V).

CV curves of $[Cu_2L]Cl_2$ at GC (Fig. 8b) demonstrate less pronounced voltammetric features as compared to those at HOPG. The reduction process C1 is detected at potentials below −0.8 V, which wave looks like two coalesced waves. With increasing the scan rate the anodic peak at 0 V (process A1) and anodic response at ca. −0.5 V (process A3) become indistinct.

Unfortunately, for the majority of data the pronounced background contributions complicate the use of traditional quantitative tests based on the scan rate dependence. In general, for C1 a linear current dependence on a square root of scan rate is found, with non-zero intersect at ordinate. The latter most probably corresponds to hydrogen evolution. This dependence favours an assumption that process C1 corresponds to reduction of dissolved $[Cu_2L]Cl_2$ with mass transfer control.

Electrochemical behaviour of immobilized $[Cu_2L]Cl_2$

The reduction of $[Cu_2L]Cl_2$ dissolved in aqueous solution seems to consist of several elementary steps, and is likely to be complicated by adsorption of complex or reduction products at the electrode surface. This assumption results from the following general observations: (1) The formation of copper adlayer at gold electrode in the course of $[Cu_2L]Cl_2$ reduction demonstrates saturation at submonolayer coverages, which natural reason can be coadsorption with organic species. (2) Some redox features (A2, C2) are found which voltammetric behaviour complies with quasi-reversible transformations of adsorbed reactant. (3) According to our previous findings [5] the inhibition of hydrogen evolution on gold in the presence of $[Cu_2L]Cl_2$ is observed at potentials from −0.9 to −1 V. (4) The STM data give evidence of adsorbate formation and its stability on carbon support even after washing. So it is interesting to explore the redox properties of $[Cu_2L]Cl_2$ immobilized on the electrode surface.

The attempts to immobilize $[Cu_2L]Cl_2$ at polycrystalline gold electrode by dropping a portion of $[Cu_2L]Cl_2$ solution at the surface (as in the case HOPG electrode) or by holding the electrode in the solution of reactant were unsuccessful. The voltammetric responses of resulting electrode were indistinct compared to CVs for

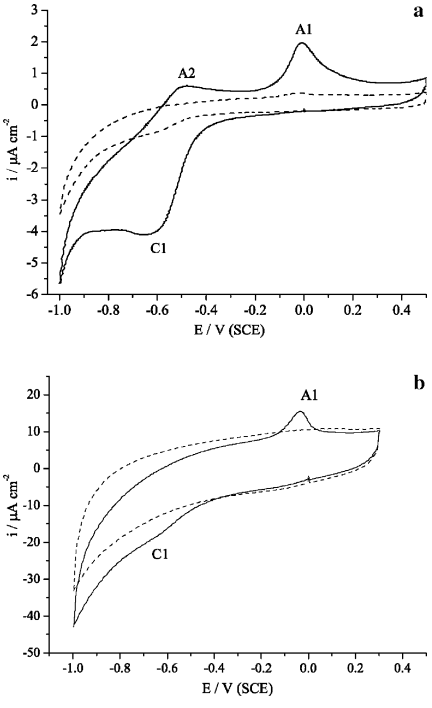

Fig. 9 Cyclic voltammograms of $[Cu_2L]Cl_2$ attached at: **a** HOPG (0.56 cm^2, 40 μl of 85 μM $[Cu_2L]Cl_2$), **b** GC electrode (1.6 cm^2, adsorption from 0.33 mM $[Cu_2L]Cl_2$); *dotted line*: cyclic voltammogram of bare **a** HOPG, **b** GC electrode. Scan rate 0.05 V s^{-1}

bare gold electrode in supporting solution, which behaviour probably results from surface reconstruction (Fig. 5c). The presence of residual redox-inactive adsorbate also cannot be ruled out.

Being immobilized at HOPG electrode surface $[Cu_2L]Cl_2$ demonstrates three specific voltammetric responses as compared to CVs of bare electrode in supporting solution (Fig. 9a). Characteristic potentials are close to the values found for some peaks (Table 1) of dissolved $[Cu_2L]Cl_2$ reduction. Peak corresponding to the process A1 is observed at CVs for immobilized reactant. The voltammetric responses at ca. −0.5 V (anodic) and −0.6 V (cathodic one) should be associated with processes A2/C2. This pair was assigned above to redox activity of surface-attached $[Cu_2L]Cl_2$. The cathodic currents are by a factor of ten lower compared to the values of currents for process C1 and those for A2/C2 at CV for dissolved reactant (Fig. 6a) at the same scan rate. At the same time the current values for A2 and C2 do not depend crucially on the presence/absence of $[Cu_2L]Cl_2$ in solution.

The estimated charge spent for the process C2 (Fig. 9a) is approximately equal to total charge of anodic responses A2 and A1 (if background cathodic contribution is taken into account). Thus, the fact that the reduction of dissolved $[Cu_2L]Cl_2$ at HOPG is really accompanied by more reversible redox transformations of adsorbed reactant is rather plausible. As follows from the existence of two anodic peaks, a major portion of C2 products forms metallic copper, when a minor portion presents another type of species. The metallic copper desorption (A1) agrees with assumption of reversible solid-state conversion of metal complex to metal deposit and free ligand, by analogy with Ref. [10]. Fig. 9a gives evidence of a parallel redox process (A2) with participation of copper containing surface-attached reactant, which can be incompletely reduced $[Cu_2L]Cl_2$ species.

The CV curve registrated at GC electrode with adsorbed $[Cu_2L]Cl_2$ is compared with CV for bare electrode in supporting solution in Fig. 9b. Voltammetric curves for $[Cu_2L]Cl_2$ attached to HOPG and GC demonstrate qualitatively similar voltammetric responses except for the fact that cathodic peak at GC is rather indistinct and broad. In contrast to the $[Cu_2L]Cl_2$ immobilized at HOPG surface, no anodic peak corresponding to process A2 at CV curves was observed for the complex adsorbed at GC electrode even with an increase of scan rate. This fact is likely to be due to low concentration of $[Cu_2L]Cl_2$ at the surface layer otherwise this means dissimilar redox features of the complex at GC and HOPG electrodes.

Arguments for hypothesis of reversible copper demetallation in the course of $[Cu_2L]Cl_2$ reduction

To compare the redox activity of $[Cu_2L]Cl_2$ in solution or being immobilized at electrode surface the following observations are to be pointed out (Table 1). For all the electrode materials the reduction process C1 and the corresponding anodic voltammetric response A1 are detected. The latter one results from metallic copper desorption.

There is no other anodic voltammetric responses outside A1 potential region for $[Cu_2L]Cl_2$ at gold electrode and the reactant being attached to GC. For both dissolved and immobilized $[Cu_2L]Cl_2$ no voltammetric response associated with aqueous copper ions reduction, which would occur in subsequent potential cycle after stripping of the metallic copper, is observed.

At high scan rates CV curves at carbon electrodes for dissolved $[Cu_2L]Cl_2$ manifest an anodic response (A3) that cannot be detected at low scan rates. This specific feature of process A3 results from chemical reaction that complicates the overall reactant reduction. If subsequent chemical reaction is possible for each electron transfer step:

$$Cu^{II}Cu^{II}L^{2+} \xrightarrow{1e^-} Cu^{I}Cu^{II}L^{+} \xrightarrow{1e^-} Cu^{I}Cu^{I}L \xrightarrow{2e^-} 2Cu_{(s)} + L$$

the redox processes observed by cyclic voltammetry includes also the responses of redox active products of chemical steps. At the cathodic scan each of one-electron or two-electron steps may contribute to the voltammetric response (C1). In the case of high scan rates, when the rate of electron transfer is supposed to exceed the rate of chemical reaction step, process A3 is likely to be an oxidation of $Cu^{II}\ Cu^{I}\ L^{+}$ or $Cu^{I}\ Cu^{I}\ L$ coupled with (C1) reduction. Both $Cu^{II}\ Cu^{I}\ L^{+}$ and $Cu^{I}\ Cu^{I}\ L$ are capable to undergo the disproportionation yielding Cu(II) ions and metallic copper which is oxidized at the anodic scan direction reverse (process A1). The disproportionation with final free ligand formation is rather plausible process taking into account the instability of $[H_4L]^{2+}$ in aqueous medium.

The hydrolysis of free ligand is likely to slow down when the reduction of $[Cu_2L]Cl_2$ attached to the HOPG electrode surface takes place. If this is the case, Cu(II) ions formed in the course of desorption (process A1) can bind with the ligand resulting in the initial $[Cu_2L]^{2+}$ species. Thus certain reversibility of chemically irreversible electroreduction of $[Cu_2L]Cl_2$ seems to be achieved by CV method in the case of reactant immobilized on carbon electrodes.

In summary, the overall $[Cu_2L]Cl_2$ reduction process at the HOPG surface does not contradict the hypothesis of copper demetallation and binuclear complex $[Cu_2L]Cl_2$ reformation during a reversal scan. However, in the presence of dissolved reactant this process is voltammetrically screened by much higher irreversible responses.

Conclusions

The binuclear complex compound $[Cu_2L]Cl_2$ demonstrates redox activity at HOPG, GC and gold electrodes in the potential range from 0.3 to −1 V being both

dissolved and immobilized on carbon materials. Copper ions involving redox transitions of $[Cu_2L]Cl_2$ seem to be complicated by subsequent chemical reactions. The chemically irreversible metallic copper formation is detected at all electrodes under discussion. In accordance to STM and CV data the binding of cuprous ions with free ligand during anodic scan is assumed to be possible in the case of $[Cu_2L]Cl_2$ immobilized on HOPG electrode. The CV data obtained for the surface-immobilized $[Cu_2L]Cl_2$ demonstrate better redox reversibility, which is interpreted in terms of higher ligand stability as compared to dissolved ligand formed in the course of demetallation in solution. These results in combination with data on the free ligand electrochemistry studied for the first time demonstrate the occurence of quasi-reversible demetallation even for dissolved complex, despite of its apparently irreversible voltammetric behaviour.

These findings do not prevent a search for mediating effects of $[Cu_2L]Cl_2$ in aqueous electrocatalysis, as despite of parallel irreversible processes the immobilized species behave reversibly.

Acknowledgements The authors would like to thank Egor Smurnii (Moscow State University) for appreciable contribution into synthesis. Russian Foundation for Basic Research (Grant 02-03-33 321a) and Council for Grants of President of Russian Federation for leading scientific schools (NSh-2089.2003.3) are acknowledged for financial support.

References

1. Robson R (1970) Inorg Nucl Chem Lett 6:125
2. Okawa H, Kida S (1971) Inorg Nucl Chem Lett 7:751
3. Pilkington NH, Robson R (1970) Aust J Chem 23:2225
4. Moutet J-C, Saint-Aman E, Ungureanu E-M (2001) Electrochim Acta 46:2733
5. Roznyatovskaya NV, Tsirlina GA, Roznyatovskii VV, Reshetova MD, Ustynuyk YuA (2004) Russ J Electrochem 40:(in press)
6. Long RC, Hendrickson DN (1983) J Am Chem Soc 105:1513
7. Gagne RR, Koval CA, Smith TJ (1979) J Am Chem Soc 101:4571
8. Mandal SK, Adhikary B, Nag K (1986) J Chem Soc Dalton Trans 6:1175
9. Nanda KK, Addison AW, Paterson N, Sinn E, Thompson LK, Sakaguchi U (1998) Inorg Chem 37:1028
10. Marken F, Cromie S, McKee V (2003) J Solid State Electrochem 7:141
11. Roznyatovskii VV, Borisova NE, Reshetova MD, Ustynuyk YuA, Alexandrov GG, Eremenko IL, Moiseev II (2004) Izvest Acad Nauk (in Russian) 6:1161
12. Black D, Blake AJ, Finn RL, Lindoy LF, Nezhadali A, Rougnaghi G, Tasker PA, Schroder M (2002) J Chem Commun 4:340
13. Vassiliev SYu, Denisov AV (2000) Zh Tekhn Fiz (in Russian) 70:100
14. Danilov AI, Molodkina EB, Polukarov YuM (2002) Russ J Electrochem 38:732
15. Baldo MA, Bragato C, Mazzocchin GA, Daniele S (1998) Electrochim Acta 43:3413